eJSSNT Regular Paper

e-Journal of Surface Science and Nanotechnology **21**, XX−XX (2023)

Citrullus Colocynthis Fruit Extract Mediated Green Synthesis of Silver Nanoparticles: The Impact of pH, Temperature, and Silver Nitrate Concentration

Banaz Shahab Haji,[a, †] Azeez Abdullah Barzinjy [b, c, ‡]

[a] *Department of Physics, College of Education, Salahaddin University-Erbil, Erbil, Iraq*
[b] *Scientific Research Center, Soran University, Kurdistan Region, Iraq*
[c] *Department of Physics Education, Faculty of Education, Tishk International University, Erbil, Iraq*
[†] *Corresponding author: banaz.shahab96@gmail.com*
[‡] *Corresponding author: azeez.azeez@soran.edu.iq*

Received: 27 August, 2022; Accepted: 20 October, 2022; J-STAGE Advance Publication: 3 December, 2022; Published: 3 December, 2022

Silver nanoparticles (Ag NPs) can be produced from various approaches including physical, chemical, and biological approaches. However, green synthesis methods are simple, efficient, and eco-friendly methods and provide relatively more stable nanoparticles. In the current investigation, Ag NPs have been synthesized utilizing *Citrullus colocynthis* fruit extract as a reducing, capping, and stabilizing agent. Then, Ag NPs were characterized through various classification methods to investigate their size, purity, stability, degree of crystallinity, structure, and optical properties. The impact of different parameters including concentration of $AgNO_3$, pH, and reaction temperature on the biosynthesized Ag NPs and corresponding surface plasmon resonance (SPR) behavior were investigated intensively. This study showed that increasing pH values cause tightening the SPR peaks, and therefore, obtaining monodisperse NPs. On the other hand, increasing the reaction temperature increased the band gap of NPs and, thus, reduced the size of NPs. However, the agglomeration state and later the stability of the biosynthesized Ag NPs are increasing with increasing the $AgNO_3$ concentration. This investigation, exceptional and unique, confirms that reaction pH, the reaction temperature, and the precursor concentration play important roles in the formation process of NPs. Through selective combination of these trio, one can produce Ag NPs with desired structural, morphological, and optical properties which can be suitable for different applications.

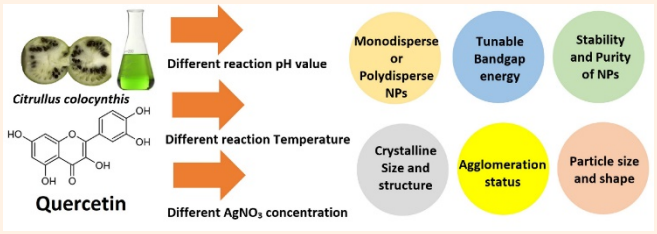

Keywords *Green synthesis method; Silver nanoparticles; Reaction pH; Citrullus colocynthis fruit extract*

I. INTRODUCTION

Recently, nanoscience has appeared as a new field of science and its applications have grown rapidly and remarkably throughout the world. Nanoscience is the investigation of constructions and performance of molecules in the nanometers size, i.e., between 1 and 100 nm [1]. On the other hand, the technology that employs the nanomaterials in real-world requests, for instance, expedients and other applications is named nanotechnology. "Nano" refers to a Greek word means "dwarf" or rather small things and means one thousand millionths of a meter (10^{-9} m) [2]. We are seeing nanotechnology offers novel technologies in various fields such as molecular diagnostics [3], drug delivery [4], imaging [5], solar cell [6], catalysis [7], and sensing [8].

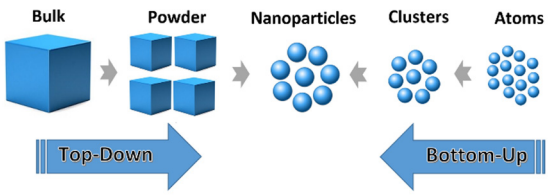

Figure 1: Top-down and bottom-up methods.

Nanoparticles (NPs) can be synthesized in general from two different approaches, i.e., "Top-Down" and "Bottom-Up" methods. Top-down approach comprises the breaking down of the bulk material into nanosized constructions or subdivisions whereas bottom-up method denotes to the accumulation of a material from the bottom: atom-by-atom, molecule-by-molecule, or cluster-by cluster (Figure 1).

Numerous preparation approaches have been employed for NPs formation together with controlling construction and dimension. Although all of these methods are capable of producing NPs, there is still a need for some improvements in the development procedures, through which good results and effective yields can be obtained. Figure 2 shows the production of NPs through numerous approaches.

NPs can be synthesized by several methods, so that physical, chemical, and biological methods are among the common methods. Choosing an environmentally friendly solvent, as a good reducing, capping and safe stabilization agents is a key factor for synthesizing NPs. Although physical and chemical approaches are superior in terms of creating stable nanostructures of uniform size, they do not achieve the goal of long-term sustainability. The biological/green method, in turn, is a safe, biocompatible, and environment-friendly method for synthesizing NPs through utilizing plants and microorganisms. Green or biological methods for synthesizing NPs can be carried out through fungi, algae, yeast, bacteria, and plants. Diverse fragments of plants such as leaves, fruits, roots, stem, seeds have been used for synthesizing numerous NPs owing to the existence of phytochemicals, which acts as reducing, capping and stabilizing agent. These phytochemicals can, also, regulate the size and morphology of the NPs which can be utilized in numerous applications.

Several factors, for example the nature of a plant extract, temperature, reaction time, reaction pH, concentration of a metal ion and plant extract are affecting the shape, dimension and stability of the NPs. Increasing pH values, for instance, leads to formation of bigger particle size with more precise crystalline sizes. This is more likely due to the available natural phytochemicals in the plant extract, which influence their aptitude to bind and reduce metal cations and anions in the sequence of NPs formation.

The green method has been used for synthesizing silver (Ag) NPs in numerous previous studies. Awwad and Salem used *Mulberry* leaf extract as a capping and reducing agents for synthesizing Ag NPs [9]. Banerjee *et al.* shows the status of synthesizing Ag NPs from extensively obtainable Indian plants [10]. Khalil *et al.* synthesized Ag NPs utilizing olive leaf extract and the investigate antibacterial activity of the Ag NPs [11]. Sun *et al.* synthesized Ag NPs utilizing tea leaf extract and then evaluated their steadiness and antibacterial activity [12]. Kamalakannan *et al.* biologically synthesized Ag NPs utilizing *Argemone mexicana* leaf extract as well as investigated their antimicrobial activities [13]. Shaik *et al.* utilized *Origanum vulgare* L. extract for synthesizing Ag NPs and investigated their microbicide activities [14]. Khan *et al.*, biosynthesized Ag NPs from plant extract, bacteria and fungi [15−17]. They have shown that the biosynthesized Ag NPs can be utilized as an operative growth inhibitor for numerous pathogenic microorganisms and appropriate to control microbial systems.

In the current investigation, *Citrullus colocynthis* fruit extract has been used for synthesizing Ag NPs. The reason behind selecting *Citrullus colocynthis* fruit extract is because *Citrullus colocynthis* fruit is very rich in oil and phytochemicals. The dominant phytochemical in this extract is flavonoids which are responsible for donating accessible hydrogen to the metallic ion, which results in zero-valent NPs when their OH groups are transformed from the enol-mold to the keto-mold.

The impact of pH, reaction temperature, and $AgNO_3$ concentration on the shape, size, optical properties, purity, and crystalline structure were investigated. The novelty of this study is that Ag NPs can be synthesized from a one-pot reaction without using any exterior stabilizing and reducing agent, which is not conceivable by means of the existing processes. This study, also, is rare and distinctive, and it demonstrates that the process of the NPs formation, in general, is not clear and there are many parameters affecting the structural, chemical, and optical properties of the NPs. Here, only the impact of pH, reaction temperature, and $AgNO_3$ concentration were investigated.

II. MATERIALS AND METHODS

A. *Citrullus colocynthis* fruit extract preparation

The *Citrullus colocynthis* fruit (Figure 3), commonly called Bitter Apple in English and locally called Guzhark,

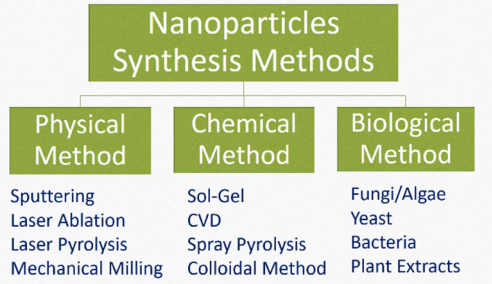

Figure 2: Representation chart for the production of NPs by numerous approaches.

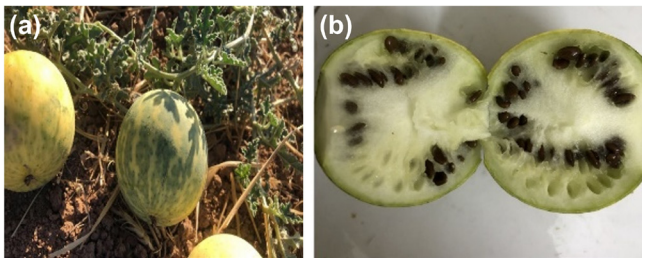

Figure 3: The photograph of *Citrullus colocynthis* fruit in (a) the field and (b) transverse half cut section.

was collected in Erbil, 36.1901° N, 43.9930° E, in the north of Iraq. The *Citrullus colocynthis* fruit extract preparation was as follows: 30 g of fresh *Citrullus colocynthis* fruit was washed using distilled water to eliminate all the dirt, cut into fine pieces, and sodden in a flask alongside with 100 mL of distilled water. The mixture was heated at 50°C for 30 min (Figure 4). After that, the mixture was permitted to cool down to room temperature and strained with a filter paper to eliminate undesirable organic materials.

B. Synthesis of silver nanoparticles

In general, this study aimed to prepare Ag NPs using a green synthesis method. *Citrullus colocynthis* fruit extract was used as reducing, capping, and stabilizing agents, and $AgNO_3$ with different concentrations (0.1−0.5 g) was used as an Ag ions source. In addition, sodium hydroxide, NaOH, was utilized to control the reaction pH. Different pH values between pH 6 and 10 was employed to study the impact of the pH on the Ag NPs. All of the utilized chemicals were purchased from Sigma Aldrich.

The preparation process of the Ag NPs was as the follows. First, 0.2 g of $AgNO_3$ was liquefied in 50 mL of double distilled water and was stirred for 20 min at 60°C. 50 mL of *Citrullus colocynthis* fruit extract solutions were added drop-by-drop to the liquefied $AgNO_3$ solution. The solutions with the pH between 6 and 10 were prepared to assess the effect of the pH. The final mixtures were heated on the hot plate and stirred at 60°C for 40 min until the color of the mixtures changed brown. The precipitates were acquired by centrifugation at 7000 rpm for 25 min, and then heated in a muffle furnace at 500°C for 40 min to eliminate all contaminants and organic materials around the Ag NPs. Second, the other samples with different pH values were prepared using the above-mentioned procedure. Third, the amount of 0.1 to 0.5 g of $AgNO_3$ was liquefied in 50 mL of double distilled water, and the solution was stirred for 20 min at 60°C. Then, 50 mL of *Citrullus colocynthis* fruit extract solutions were added dropwise to liquefied $AgNO_3$, while the pH value was fixed at pH 8 for all of the samples. The final mixtures were heated on the hot plate and were stirred at 60°C for 40 min until the color of the mixtures changed brown. The precipitates were acquired by centrifugation at 7000 rpm for 25 min and heated at 500°C for 40 min. Figure 5 shows the process for the synthesis of Ag NPs.

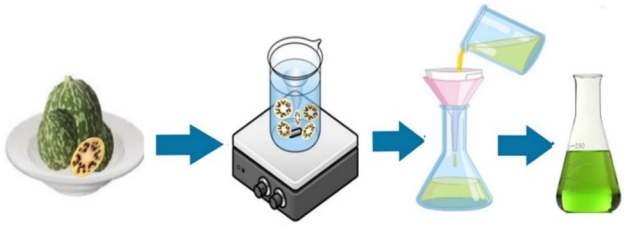

Figure 4: Preparation process of *Citrullus colocynthis* fruit extract.

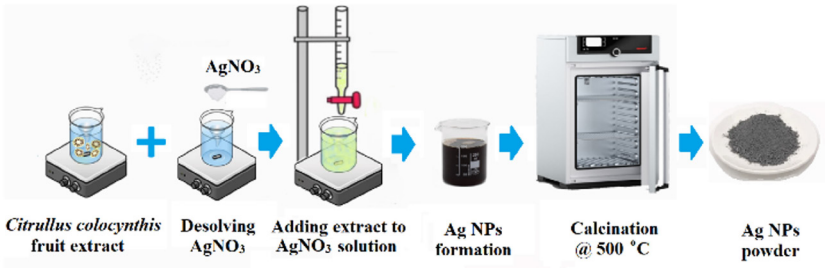

Figure 5: Schematic diagram of the Ag NPs preparation.

C. Characterization techniques

To investigate the crystalline structure of prepared Ag NPs, X-ray diffraction (XRD) (PAnalytical X' Pert PRO, Cu Kα = 1.5406 Å) was used. The skimming rate was 1° min^{-1} in the 2θ range between 20° and 80°. In addition, the optical properties of the Ag NPs samples were studied utilizing the double beam ultraviolet-visible (UV-Vis) spectrometer (Super Aquarius Spectrophotometer-1000) with a deuterium and tungsten iodine lamp in the range of 200 to 900 nm at room temperature. Morphology of the samples were studied through the scanning electron microscopy (SEM) (Quanta 450). The elemental composition of the Ag NPs was determined by energy-dispersive X-ray spectroscopy (EDX) implemented in the SEM instrument. The composition and organic molecules around the Ag NPs were analyzed using Fourier-transform infrared (FTIR) (Perkin Elmer) spectrophotometer in the acquisition range of 400−4000 cm^{-1}.

III. RESULT AND DISCUSSION

A. Characterization of *Citrullus colocynthis* fruit extract

1. UV-Vis analysis

UV-Vis absorption spectroscopy is the most widely used technique, which is useful for pre-identification of the available phytochemicals in the utilized fruit extract. Most of the available phytochemicals in the plant extracts can be screened at a wavelength range between 200 and 400 nm. These phytochemicals can be utilized as reducing, capping, and stabilizing agents for the fabrication of the Ag NPs. These phytochemicals have active functional groups, such as hydroxyl, aldehyde, and carboxyl units, which are playing essential parts in providing synergistic chemical reduction power for the reduction of Ag ions into Ag^0.

Many studies reported the presence of various phytochemicals in *Citrullus colocynthis* fruit [15, 16]. The qualitative and quantitative analysis documented that flavonoid in *Citrullus colocynthis* fruit extracts is probably the

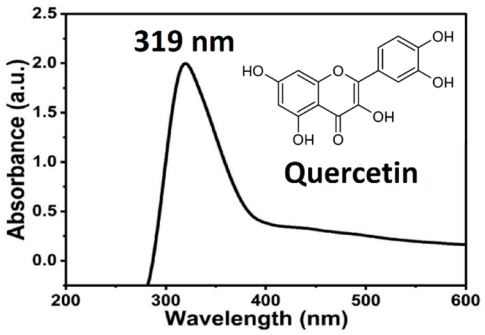

Figure 6: UV-Vis spectra for *Citrullus colocynthis* fruit extract.

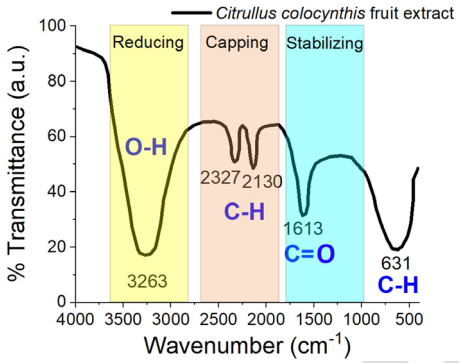

Figure 7: FTIR spectrum of *Citrullus colocynthis* fruit extract.

dominant available phytochemical. Figure 6 show the UV-Vis spectra of *Citrullus colocynthis* fruit extract. *Citrullus colocynthis* fruit extract possesses a maximum UV peak at 319 nm. This peak is most likely associated to quercetin, a plant flavanol from the flavonoid group. As show in the inset of Figure 6, quercetin possesses several OH groups which are responsible for reducing Ag ions to zero-valent Ag, while the other groups are responsible for capping and stabilizing the Ag NPs [17].

2. FTIR analysis

FTIR spectroscopy was utilized to determine the functional group present in the fruit extract. An FTIR spectrum commonly have two regions; the functional group region (1800−4000 cm^{-1}) and the fingerprint region (0−1500 cm^{-1}). The FTIR spectrum for *Citrullus colocynthis* fruit extract is shown in Figure 7. *Citrullus colocynthis* fruit extract exhibits several peaks between 4000 and 400 cm^{-1}.

It is known that the synthesis of NPs using green methods can be, in general, done through three different stages: First, the available phytochemicals in *Citrullus colocynthis* fruit extract, precisely the OH groups (Figure 7), involve in in the Ag^{+}-to-Ag^{0} reduction. This stage is known as a reducing stage. In our case, the peak at 3263 cm^{-1} is attributed to the O−H stretching and, compared with other peaks, it is the most intense and broad peak. This is not surprising, since the UV-Vis analysis showed that *Citrullus colocynthis* fruit extract contains the quercetin compound which has several OH groups. One of the advantages of the green synthesis method is that, in many cases, a reducing agent behaves simultaneously as a capping agent. Therefore, the necessity for an exterior capping agent is omitted. The second stage is the nucleation and growth stage, where the reduced Ag^{0} atoms agglomerate to form the NPs. A piece of the material nucleates and grows in response to its reaction conditions, while a minor change of the condition, for instance the solution pH, can cause an entirely different mechanism [18]. The peak at 2130 cm^{-1} is assigned to the C−H stretching, indicating the capping agent in the plant extract. The final stage is the stabilization stage. Here, the available secondary metabolites in the extract are responsible for the stabilization of the NPs. In general, the green synthesized NPs are more stable than the other NPs synthesized by the traditional methods. The peak at 1613 cm^{-1} corresponds to the C=O group. This peak represents the stabilizing agent in the plant extract. The comprehensive mechanism of formation of the Ag NPs using plant extract can be found in our previous investigation [19]. Different sizes and shapes of metallic NPs can be effectively produced by means of phytochemicals by varying the producing factors of the pH, the temperature, the incubation time, and the slat/plant concentration.

B. Characterization of green synthesized Ag NPs

1. UV-Vis analysis

The reaction pH of the mixture, i.e., the Ag ion solution and the plant extract, has a great impact on the synthesizing process of the Ag NPs. Formation of the Ag NPs was examined at different pH values by changing the amount of added NaOH to the mixture. The pH of the suspension was monitored by the end-point of the reaction. The reaction pH affects morphology and dimension of the NPs and, thereby, UV-Vis absorption spectra of the Ag NPs. This can be explained, since inadequate protection of the NPs surface causes the larger NPs formation but with improved crystallite sizes. In this study, the pH values of 6, 7, 8, 9, and 10 were chosen to study the effect of pH on morphology, size, band gap, crystalline size, pureness, and steadiness of the green synthesized Ag NPs using *Citrullus colocynthis* fruit extract. The reaction temperature and the time were fixed at 60°C and 50 min, respectively, during these reactions.

Figure 8(a) shows UV-Vis absorption spectra at different pH values. The peak maxima are 440, 441, 441.8, 442, and 444 nm for pH 6, 7, 8, 9, and 10, respectively. Surprisingly, the peak maximum shifts towards the longer wavelength side with increasing the reaction pH value. Singh *et al.* [20] stated that the biosynthesized Ag NPs at different pH values show a different surface plasmon resonance (SPR) behavior. The current study showed that the increase of the pH value resulted in narrowing of the SPR peaks. This is a clear indicator for obtaining monodisperse NPs at higher pH values. Further increase in the reaction pH to 10 causes an increase in the SPR peak intensity, which is considerably narrowed and red-shifted to about 444 nm. This, in turn, can be clari-

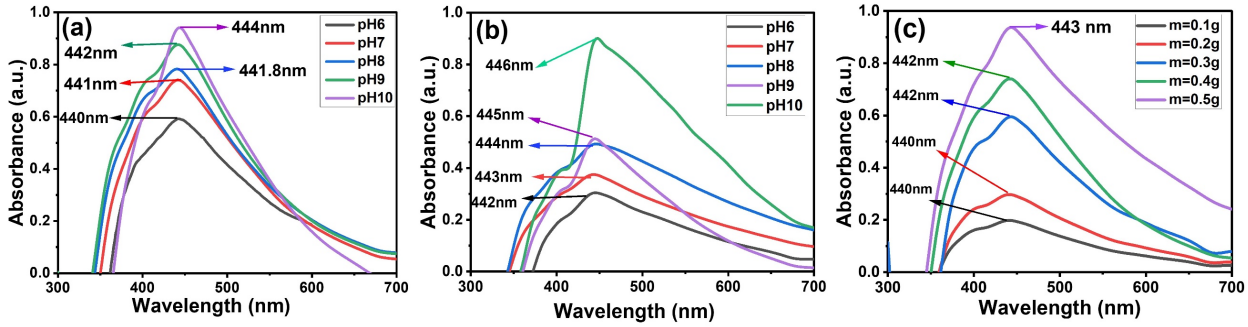

Figure 8: UV-Vis spectra of the green synthesized Ag NPs at various pH values (6−10) at 60°C (a) and 70°C (b) and with various metal ion concentrations (0.1−0.5g) at pH 10 and 60°C (c).

fied, because increasing the reaction pH by adding NaOH would provide more ions to the medium and, thus, increase the rate of reduction of metal ions. The higher reduction rate of metal ions causes the creation of larger particles in the medium and, thus, the redshift occurs. The outcomes of this study allow a better view of how the pH affects the formation of the Ag NPs in the reaction with *Citrullus colocynthis* fruit extract. We show how the reaction rate is altered with pH and, hence, how the SPR peak position, the size, and the shape of the NPs change. This will allow to more accurately determine the effect of pH on this type of the reaction and to obtain colloids of a precise size. On the other hand, the hyperchromic shift within increasing the NPs size can be attributed to the size dependence of the sprinkling rate of the conduction electrons on the surface of the NPs [21]. Moreover, as the NPs size increases, the sprinkling rate of the conduction electrons decreases and the SPR wavelength increases. Similar results have been reported by many researchers [22, 23].

Figure 8(b) shows UV-Vis absorption spectra at various pH values at 70°C. The impact of increasing the reaction temperature is obvious, leading extra redshifts of the SPR peaks. The peak maxima are 442, 443, 444, 445, and 446 nm for the pH values of 6, 7, 8, 9, and 10, respectively. Numerous studies highlighted the clear impact of the temperature on the shape, the size, and morphology of NPs [24, 25]. The present investigation showed that increasing the reaction temperature could also accelerate the NPs formation reaction. Increasing the reaction temperature leads to increasing the band gap of NPs and, hence, decreasing the NPs size. This is more likely due to the increase of the reduction rate of the Ag^+ ions, which is followed by homogenous nucleation of the Ag atoms. The process of increasing the temperature of the reaction is not absolute because we are talking about the nanoscale, incredibly sensitive to an unimaginable degree. Moreover, there are many factors that interfere the increase of the system temperature, or in other words, the system's entropy. The evaporation of the mixture must be also taken into account because the mixture is aqueous and contains a large amount of water [26].

Figure 8(c) shows UV-Vis absorption spectra using 50 mL of *Citrullus colocynthis* fruit extract at 60°C and pH 10 with different $AgNO_3$ concentrations of 0.1, 0.2, 0.3, 0.4, and 0.5 g. Increasing the concentration of the metal ion

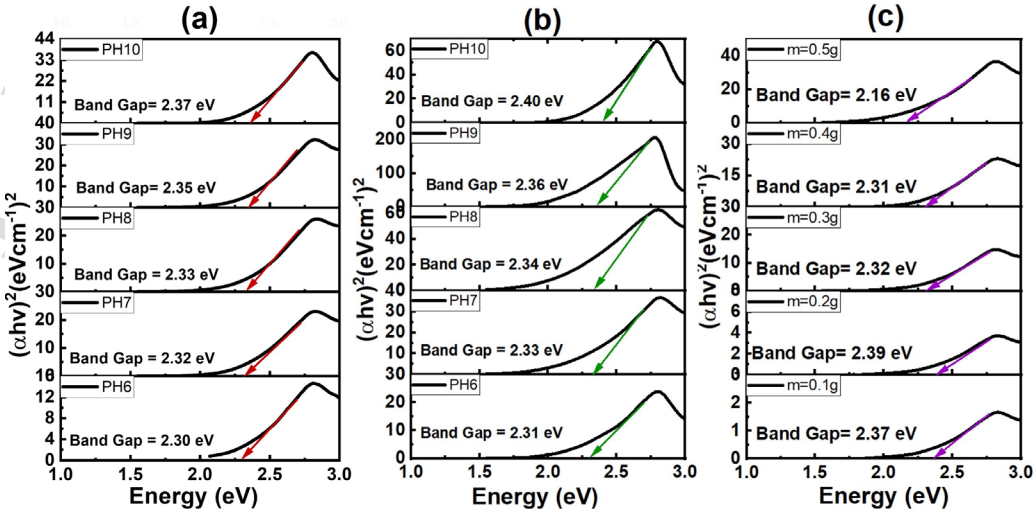

Figure 9: Energy band gap of the Ag NPs at various pH values (6−10) at 60°C (a) and 70°C (b) and with different metal ion concentrations (0.1−0.5g) at 60°C and pH 10 (c).

leads to an increase in the particle size, which will be discussed later in the SEM analysis. The maximum SPR wavelength is obtained at the highest concentration, i.e., 0.5 g $AgNO_3$. Moreover, the highest concentration gives the peak with highest absorbance. On the other hand, the concentration of the metal ions has a clear impact on the broadness of the absorption peaks, due to the formation of the polydisperse Ag NPs. This is explainable because the availability of more metal ions in the medium with a fixed amount of the OH groups lead to uncontrollable nucleation and growth and, hence, formation of polydisperse NPs. Another consequence is that the higher $AgNO_3$ concentration would result in the increase in the agglomeration state and, hence, the stability of the biosynthesized Ag NPs. Similar results have been reported by other researchers [27, 28].

The energy band gap of the green synthesized Ag NPs was evaluated by the Tauc plot by assuming the lined ratio of the UV-Vis curve. Figure 9 shows the effect of changing the reaction pH, the temperature, and the metal ion concentration on the band gap of the green synthesized Ag NPs using *Citrullus colocynthis* fruit extract. The increase in the reaction pH leads to the increase in the band gap of the NPs [Figure 9(a, b)]. This was predictable because the pH has a great impact on the size of the NPs and because the energy band gap depends largely on the size. In general, the energy band gap of the NPs is affected by various parameters such as the composition of NPs, the phase construction, particle dimension, surface functional groups, crystallinity, surface defects, and so on. Figure 9(b) indicates that the band gap increases with increasing the reaction temperature from 60 to 70°C if the solution pH is maintained. This is more likely due to the fact that the NPs size decreases with increasing the reaction temperature. In a similar study, Kaviya *et al.* [29] observed, using the orange peels for synthesizing Ag NPs, the influence of the temperature on the size of the NPs. They discovered that 35 nm Ag NPs were synthesized at approximately 25°C and that the size of the Ag NPs was reduced to 10 nm after increasing the reaction temperature. Moreover, Park *et al.* [30] found that higher temperatures led to the consumption of more metal reactants and faster production of smaller NPs.

Figure 9(c) shows the impact of the $AgNO_3$ concentration on the band gap of biosynthesized Ag NPs at 60°C and pH 10. Five different concentrations from 0.1 to 0.5 g were examined. The trend is relatively different; the band gap increases from 0.1 to 0.2 g, while it decreases dramatically from 0.3 to 0.5 g. The decrease in the band gap is related to the increase in the particle size. This can be explained as a result of the presence of the defect-induced energy levels among the conduction and valence bands, more explicitly the energy levels not far from the conduction band. These narrow levels can reduce the actual band gap for minor particles, if their density is higher.

2. FTIR analysis

FTIR spectroscopy was originally utilized to observe the functional groups that bonded on the Ag NPs surface and were involved in the creation of the Ag NPs. Figure 10 shows the FTIR spectra between 4000 and 500 cm^{-1} of the Ag NPs synthesized by *Citrullus colocynthis* fruit extract at different conditions. It is seen from Figure 10(a, b) that the band at around 3500 cm^{-1}, which corresponds to the O−H stretching vibrations, depends on the pH. Otherwise stated, the increase of the reaction pH value leads to decreasing the broadness of this peak. This result is consistent with the UV-Vis analysis, since the higher reaction pH value produces smaller NPs and, hence, less OH groups on the surface. Similar analysis results have been obtained in previous studies [31−33]. On the other hand, the broad O−H stretching vibrations are obtained with 0.1, 0.3, and 0.5 g $AgNO_3$ concentrations (Figure 10c). This trend is totally different from that with 0.2 and 0.4 g $AgNO_3$. A weak band at around 2900 cm^{-1} corresponds to C−H stretching of alkanes [34]. It appears that this peak is neither affected by the reaction pH values nor by the $AgNO_3$ concentration. This is more likely

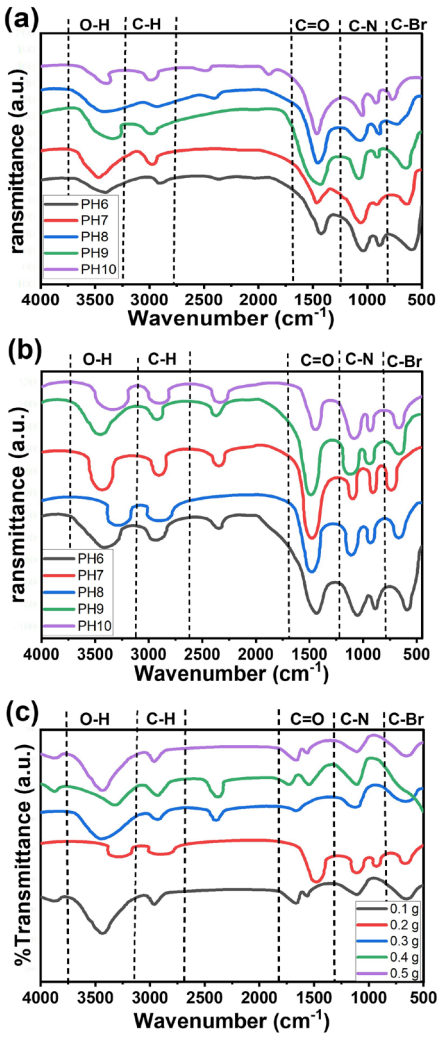

Figure 10: FTIR spectra of the biosynthesized Ag NPs at various pH values (6−10) 60°C (a) and 70°C (b) and with different metal ion concentrations (0.1−0.5g) at 60°C and pH 10 (c).

due to the nature of the C−H bond. According to the FTIR analysis of *Citrullus colocynthis* fruit extract (Figure 7), this band corresponded to the capping agent. Therefore, the agglomeration state is almost the same in all of the reaction pH values and the $AgNO_3$ concentrations. This can be further discussed in the SEM analysis section (Section III.B.4). The strong band at around 1500 cm^{-1} [Figure 10(a, b)] is assigned to C=O stretching and is also less affected by changing the reaction pH values. As have mentioned in Figure 7, this band is associated with the stabilizing agents. The appearance of this band with this clarity is a good indicator that the synthesized Ag NPs are stable regardless the reaction pH vales. However, the impact of the $AgNO_3$ concentration on this peak [Figure 10(c)] is different; the peak became broader at 0.2 g $AgNO_3$ concentration, whereas an extra tiny peak appeared at the larger wavenumber side when 0.1, 0.4, and 0.5 g $AgNO_3$ concentrations were utilized. This is probably the decrease in the constancy of the Ag NPs within these conditions. This will be supplementary discussed in Section III.B.4. The peaks around 1000 cm^{-1} designate the existence of C−N stretch aliphatic amines. These band are, more or less, affected by the reaction pH values [Figure 10(a, b)]. On the other hand, in the case of changing the $AgNO_3$ concentration [Figure 10(c)], these two peaks are merged to a single peak at the concentrations other than 0.2 g. This is probably owing to providing more nitrogen atoms to the reaction medium and, hence, forming stronger C−N stretch peaks. The peak at around 600 cm^{-1} belongs to the C−Br stretching vibration, representing the alkyl halides group.

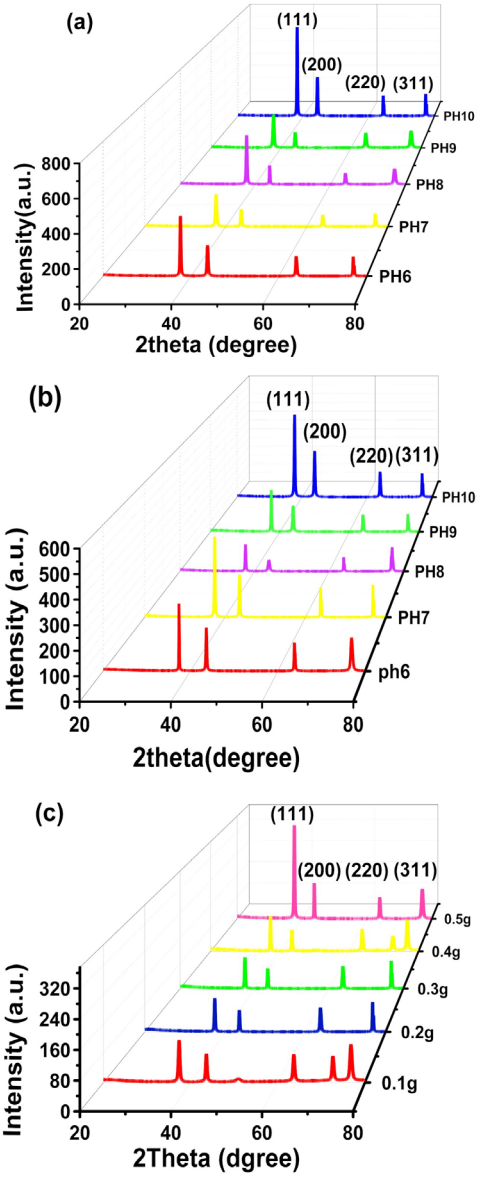

Figure 11: XRD patterns of the green synthesized Ag NPs at various pH values (6−10) at 60°C (a) and 70°C (b) and with different metal ion concentrations (0.1−0.5g) at 60°C and pH 10 (c).

3. XRD analysis

To classify the crystalline dimension and structure of the green synthesized Ag NPs, XRD analysis was implemented in the 2θ angles range between 20° and 80°. Figure 11 shows that all samples possess, regardless of the reaction pH value and the concentration on the $AgNO_3$ precursor, four diffraction peaks at 38.01°, 44.34°, 65.52°, and 77.30°, which are related to (111), (200), (220), and (311) planes of Ag NPs, respectively. The lattice constant measured from this arrangement has been estimated to be a = 4.0850 Å, which is close to the typical value a = 4.0686 Å from the JCPDS file No. 04-0783. According to these (*hkl*) planes of the crystal, there is the supplementary indication that Ag is crystallized in the face-centered cubic structure. The results of this study were consistent with the previously reported investigations [19, 35]. The average crystalline size of the Ag NPs can be calculated using the Debye-Scherrer formula: $D = K\lambda/(\beta \cos\theta)$, where K is the Scherrer constant with values of 0.9−1 (the shape factor), λ is the X-ray wavelength, β is the full width at half maximum of the XRD peaks, and θ is the Bragg angle. The regular crystalline dimension of the Ag NPs for different reaction pH values at 60°C were around 54, 48, 42, 41, and 34 nm for the pH vales of 6, 7, 8, 9, and 10, respectively [Figure 11(a)]. On the other hand, the average sizes at 70°C were about 50, 43, 39, 36, and 24 nm for the pH vales of 6, 7, 8, 9 and 10, respectively [Figure 11(b)]. The average crystalline size of the Ag NPs for the different $AgNO_3$ concentrations at 60°C and pH 10 were around 31, 23, 39, 44, and 44 nm for the $AgNO_3$ concentrations of 0.1, 0.2, 0.3, 0.4, and 0.5 g, respectively [Figure 11(c)]. It is worth noticing that the difference between the XRD spectra in Figure 11(c) and those in Figure 11(a, b) is extra XRD peaks with the $AgNO_3$ concentrations of 0.1 g and 0.4 g. This is more likely owing to the contribution of other compounds that are formed within these concentrations and have a crystalline structure. It can be stated that the (111) plane is dominant in all cases and possesses the highest intensity. This is the clear indicator that the orientation of the crystal growth is mainly along the (111)

plane.

The correlation between the XRD analysis (Figure 11) and the FTIR analysis (Figure 10) indicates that the smaller abundance of the OH group in various pH at 60 and 70°C with different metal ion concentrations leads to the formation of the exotic peaks in the XRD spectrum. These exotic peaks, precisely with the 0.1 and 0.4 g salt concentrations, are more likely belong to $AgNO_3$ rather than the formation of Ag NPs.

4. SEM analysis

The average particle dimension of the resultant Ag NPs samples and surface morphology of the particles have been studied utilizing the SEM analysis. The Ag NPs were produced by using *Citrullus colocynthis* fruit extract as reducing, capping, and stabilizing agents at different reaction pH, reaction temperature, and $AgNO_3$ concentrations. Figure 12 shows SEM images of the Ag NPs for the above-mentioned conditions. It can be easily observed that, apart from pH 6, the particle sizes of the Ag NPs are in nanoscale. Surprisingly, even after increasing the reaction temperature to 70°C, the particle sizes are still above the standard range of nanoparticles, i.e., 1−100 nm, at pH 6. Unattainability of the precise particle size at pH 6 to the reaction temperatures of 60 and 70°C is most probably due to the insufficient number of the reducing agents and, hence, the particle size is beyond the required limit [20]. It can be noticed from the regular particle dimension histogram utilizing the imageJ software that the average size of the particles at pH 6 is approximately 134 and 107 nm at 60 and 70°C, respectively. Figure 12 also shows that, at the reaction temperatures of 60 and 70°C, the average particle size is reduced with increasing the reaction pH vales. However, this size reduction is more noticeable at 70°C than 60°C. This is more likely due to the acceleration in the reduction process and, hence, the formation of relatively smaller NPs. The combination between the pH and the temperature determines the size and the shape of these NPs, suggesting the importance of the role of thermal agitation in the efficiency of the nucleation process and the growth of NPs [36]. In general, the Ag NPs are stable under pH 8 and they start to agglomerate at the pH greater than 8. This is more likely due to the functional obstruction of biomolecules, mainly proteins, which can effortlessly adapt the NPs surface characteristics and prevent them from agglom-

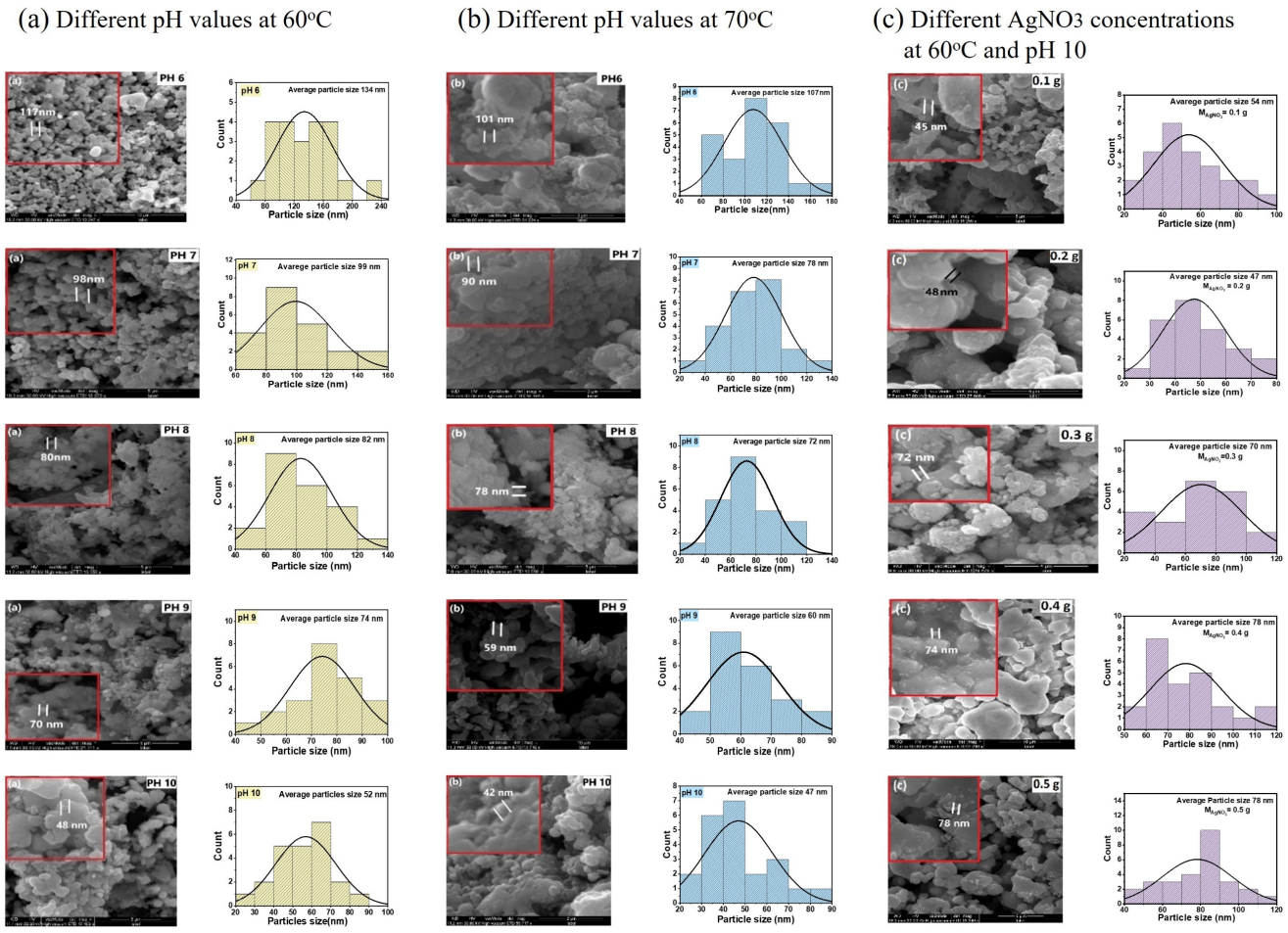

Figure 12: SEM images of the Ag NPs at different pH values at 60°C (a) and 70°C (b) and with different $AgNO_3$ concentrations at 60°C and pH 10 (c).

eration. Accordingly, the temperature increase leads to an increase in both the plasmonic bands and the rate of formation of NPs. This feature is characteristic of the formation of NPs, which leads to the decrease in their average size, given by the contribution that the nucleation rate of NPs increases with temperature. These consequences specify that the influence of temperature not only impacts the reaction rate but also affects the morphologies of the Ag NPs in the plasmonic mediated reaction. Another important point, which should be highlighted here, is that the reaction temperatures were fixed at 60 and 70°C. This can be directly related to the formation of the spherical shape of the Ag NPs. This, in turn, might be explained utilizing the Gibbs free energy, $\Delta G = \Delta H - T\Delta S$, where ΔH is the enthalpy change and ΔS is the entropy alteration. The spherical Ag NPs possess a higher surface area to the volume ratio than the other shapes and, therefore, it is more likely to generate smaller entropy and smaller heat of formation. The precise reaction at a low temperature causes the spherical NPs, because $|\Delta H|$ is greater than $|T\Delta S|$ at lower temperatures. Conversely, the reaction at a high temperature results in the formation of none-spherical NPs, because $|T\Delta S|$ is greater than $|\Delta H|$ at higher temperatures [37].

We have shown that the monodispersed NPs can be pro-

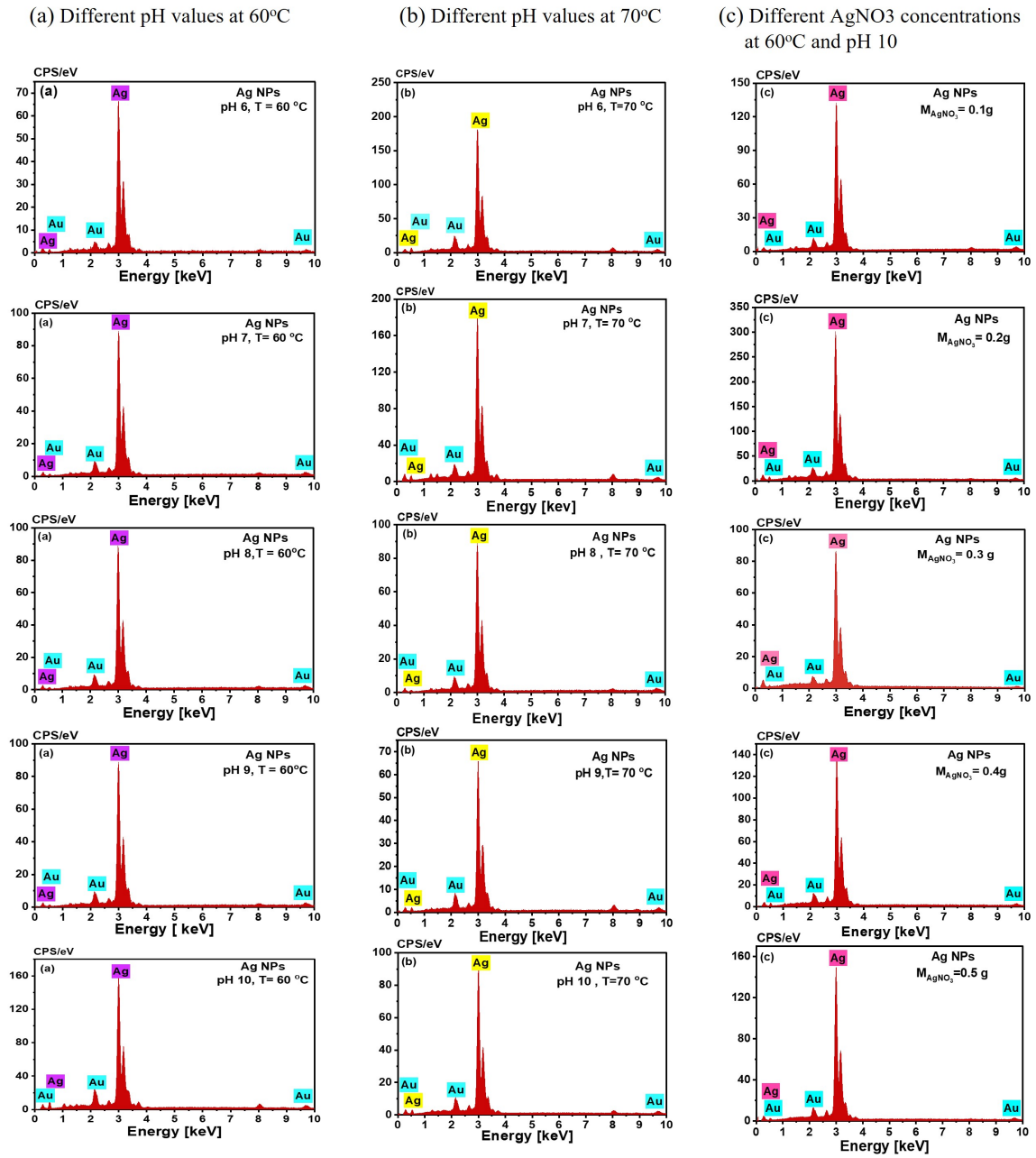

Figure 13: EDX analysis of the Ag NPs at different pH values at 60°C (a) and 70°C (b) and with different $AgNO_3$ concentrations at 60°C and pH 10 (c).

duced when the reaction temperature is 60°C and that the polydisperse NPs are formed at 70°C (Figure 8). This is most probably due to the acceleration of the nucleation rate and thus the provision of different sized NPs.

The SEM analysis [Figure 12(a, b)] confirms these results and the agglomeration state is more noticeable at 70°C than 60°C. This is extremely important, because we can control the NPs with desired shapes and sizes by adjusting these parameters. The average particles size ranges between 134 and 52 nm at the pH values between 6 and 10 at 60°C [Figure 12(a)] and between 107 to 47 nm at the pH values between 6 to 10 at 70°C [Figure 12(b)]. Figure 12(c) describes the impact of the $AgNO_3$ concentration on the dimension and morphology of the biosynthesized Ag NPs at pH 10 and 60°C. It can be noticed that the average particles size is highly affected by the precursor concentration. Similar results have been found by Manosalva *et al.* [38]. Our results indicate that the increase in the $AgNO_3$ concentration leads to the increase in the particles size. This is probably due to more Ag ions in the reaction medium so that the nucleation and growth rates increases and, hence, the particle size increases. This result is, in turn, in an excellent agreement with the previously studies [39]. Another important point one can observed from Figure 12(c) is that the agglomeration state is, relatively, higher comparing with those in Figure 12(a, b). This is again related to the inconsistent number of the Ag ions with the reducing agents which leads to uncontrollable nucleation and growth process. Figure 12(c) shows that the average particles size ranges between 54 and 78 nm for the $AgNO_3$ concentrations between 0.1 and 0.5 g at pH 10 and 60°C.

The correlation between the structural XRD analysis (Figure 11) and morphological SEM analysis (Figure 12) indicates that the Ag NPs synthesized at various pH at 60 and 70°C possesses higher degree of crystallinity than the Ag NPs synthesized at different metal ion concentrations. Thus, the foreign peaks, which belong to $AgNO_3$ rather than the Ag NPs, are responsible for the irregular nucleation and growth process and, hence, the increase in the degree of agglomeration.

5. EDX analysis

The elemental composition of the green synthesized Ag NPs was studied by the EDX analysis (Figure 13). This characterization is also significant because it provides the purity of the green synthesized Ag NPs. The energy of characteristic X-rays allows qualitative analysis to verify the elements that consist the sample, and the quantitative analysis is possible from the X-ray intensity to evaluate the amounts of the composite elements. For almost all the samples, silver and gold exit in the samples. The only significant difference among the samples prepared by different conditions is the peak intensity. The higher the intensity, the smaller the particle size, and this can be clearly noticed in all cases. According to Figure 13, the quality of the Ag NPs is high and there is no mentionable contamination in the samples. The existence of gold in all samples is owing to the SEM sample preparation; the samples were coated with a very thin layer of gold (100 Å) to improve the quality of the SEM images. Analogous analysis has been found in a previously reported investigation [40].

IV. CONCLUSIONS

In this investigation, Ag NPs were synthesized effectively through a green method utilizing *Citrullus colocynthis* fruit extract as reducing, capping, and stabilizing agents. The synthesis of the Ag NPs was carried out at different reaction pH values, different reaction temperatures, and different precursor concentrations. Various characterization techniques have been employed to study morphology, purity, crystallinity, and structural and optical properties of the biosynthesized Ag NPs. It was found that, at 60°C, the increase in the pH values led to narrowing the SPR peaks and, hence, obtaining monodisperse NPs at higher pH values. On the other hand, the increase in the reaction temperature led to increasing the band gap of the NPs and, hence, decreasing the NPs size. Moreover, the increase in the concentration of $AgNO_3$ led to increasing the agglomeration state and, hence, the stability of the biosynthesized Ag NPs. The FTIR analysis confirms that *Citrullus colocynthis* fruit extract is a good medium for synthesizing the Ag NPs, since it acts as reducing, capping, and stabilizing agents. The XRD analysis reveals that the biosynthesized Ag NPs are crystallized in the face-centered cubic structure and possess high crystallinity. Also revealed in this study is that the average crystalline size of the Ag NPs for different reaction pH values decreases with increasing the pH vales at both 60 and 70°C. Meanwhile, the average crystalline size increases with increasing the $AgNO_3$ concentrations. The SEM analysis shows that the average particle size decreases with increasing the reaction pH vales at 60 and 70°C. However, this decrease is more noticeable at 70°C than 60°C. It is also revealed that *Citrullus colocynthis* fruit extract within selected pH and temperature values can produce spherical Ag NPs, which possess a higher surface-to-volume ratio than the other shapes and, therefore, it is more likely to generate a lower entropy and a lower heat of formation. The EDX analysis showed that the quality of the Ag NPs is high and there is no mentionable contamination in the samples.

Acknowledgments

The authors would like to thank Salahaddin University-Erbil and Scientific Research center at Soran University, for their unrestricted engorgements. A special thank goes to Dr. David M. W. Waswa at Tishk International University for his excellent proofreading of this manuscript.

References

[1] B. Bocca, S. Caimi, O. Senofonte, A. Alimonti, and F. Petrucci, Sci. Total Environ. **630**, 922 (2018).

[2] F. Findik, Period. Eng. Nat. Sci. **9**, 62 (2021).
[3] B.-H. Kang, Y. Lee, E.-S. Yu, H. Na, M. Kang, H. J. Huh, and K.-H. Jeong, ACS Nano **15**, 10194 (2021).
[4] N. Desai, M. Momin, T. Khan, S. Gharat, R. S. Ningthoujam, and A. Omri, Expert Opin. Drug Deliv. **18**, 1261 (2021).
[5] Y.-C. Huang, T.-H. Chen, J.-Y. Juo, S.-W. Chu, and C.-L. Hsieh, ACS Photonics **8**, 592 (2021).
[6] Sachchidanand and D. P. Samajdar, Sol. Energy **190**, 278 (2019).
[7] A. Sápi, T. Rajkumar, J. Kiss, Á. Kukovecz, Z. Kónya, and G. A. Somorjai, Catal. Lett. **151**, 2153 (2021).
[8] H. Haick, J. Phys. D **40**, 7173 (2007).
[9] A. M. Awwad and N. M. Salem, Nanosci. Nanotechnol. **2**, 125 (2012).
[10] P. Banerjee, M. Satapathy, A. Mukhopahayay, and P. Das, Bioresour. Bioprocess. **1**, 3 (2014).
[11] M. M. H. Khalil, E. H. Ismail, K. Z. El-Baghdady, and D. Mohamed, Arab. J. Chem. **7**, 1131 (2014).
[12] Q. Sun, X. Cai, J. Li, M. Zheng, Z. Chen, and C.-P. Yu, Colloids Surf. A **444**, 226 (2014).
[13] S. Kamalakannan, S. Ananth, K. Murugan, K. Kovendan, M. Ramar, P. Arumugam, B. Chandramohan, and V. Balachandar, Curr. Pharm. Biotechnol. **17**, 1285 (2016).
[14] M. Shaik, M. Khan, M. Kuniyil, A. Al-Warthan, H. Alkhathlan, M. Siddiqui, J. Shaik, A. Ahamed, A. Mahmood, M. Khan, and S. Adil, Sustainability **10**, 913 (2018).
[15] M. Ahmed, M. Ji, P. Qin, Z. Gu, Y. Liu, A. Sikandar, M. F. Iqbal, and A. Javeed, Appl. Ecol. Environ. Res. **17**, 6961 (2019).
[16] A. I. Hussain, H. A. Rathore, M. Z. A. Sattar, S. A. S. Chatha, S. D. Sarker, and A. H. Gilani, J. Ethnopharmacol. **155**, 54 (2014).
[17] M. Škerget, P. Kotnik, M. Hadolin, A. R. Hraš, M. Simonič, and Ž. Knez, Food Chem. **89**, 191 (2005).
[18] N. T. K. Thanh, N. Maclean, and S. Mahiddine, Chem. Rev. **114**, 7610 (2014).
[19] R. F. Talabani, S. M. Hamad, A. A. Barzinjy, and U. Demir, Nanomaterials **11**, 2421 (2021).
[20] M. Singh, I. Sinha, and R. K. Mandal, Mater. Lett. **63**, 425 (2009).
[21] A. Ebrahiminezhad, S. Taghizadeh, A. Berenjian, F. H. Naeini, and Y. Ghasemi, Nanosci. Nanotechnol. Asia **7**, 104 (2017).
[22] A. K. Mittal, A. Kaler, and U. C. Banerjee, Nano Biomed. Eng. **4**, 118 (2012).
[23] P. Velmurugan, K. Anbalagan, M. Manosathyadevan, K.-J. Lee, M. Cho, S.-M. Lee, J.-H. Park, S.-G. Oh, K.-S. Bang, and B.-T. Oh, Bioprocess Biosyst. Eng. **37**, 1935 (2014).
[24] J. Huang, L. Lin, Q. Li, D. Sun, Y. Wang, Y. Lu, N. He, K. Yang, X. Yang, H. Wang, W. Wang, and W. Lin, Ind. Eng. Chem. Res. **47**, 6081 (2008).
[25] A. D. Dwivedi and K. Gopal, Colloids Surf. A **369**, 27 (2010).
[26] E. E. Elemike, D. C. Onwudiwe, O. Arijeh, and H. U. Nwankwo, Bull. Mater. Sci. **40**, 129 (2017).
[27] L. B. Anigol, J. S. Charantimath, and P. M. Gurubasavaraj, Org. Med. Chem. Int. J. **3**, 124 (2017).
[28] M. Ndikau, N. M. Noah, D. M. Andala, and E. Masika, Int. J. Anal. Chem. **2017**, 8108504 (2017).
[29] S. Kaviya, J. Santhanalakshmi, and B. Viswanathan, Mater. Lett. **67**, 64 (2012).
[30] J. Park, J. Joo, S. G. Kwon, Y. Jang, and T. Hyeon, Angew. Chem. Int. Ed. **46**, 4630 (2007).
[31] L. Rastogi and J. Arunachalam, Mater. Chem. Phys. **129**, 558 (2011).
[32] B. Kumar, K. Smita, Y. Angulo, and L. Cumbal, J. Clust. Sci. **27**, 703 (2016).
[33] S. Jain and M. S. Mehata, Sci. Rep. **7**, 15867 (2017).
[34] Md. M. O. Rashid, J. Ferdous, S. Banik, Md. R. Islam, A. H. M. M. Uddin, and F. N. Robel, BMC Complement. Altern. Med. **16**, 242 (2016).
[35] A. Roy, O. Bulut, S. Some, A. K. Mandal, and M. D. Yilmaz, RSC Adv. **9**, 2673 (2019).
[36] A. Zuorro, A. Iannone, S. Natali, and R. Lavecchia, Processes **7**, 193 (2019).
[37] S.-W. Lee, S.-H. Chang, Y.-S. Lai, C.-C. Lin, C.-M. Tsai, Y.-C. Lee, J.-C. Chen, and C.-L. Huang, Materials **7**, 7781 (2014).
[38] N. Manosalva, G. Tortella, M. Cristina Diez, H. Schalchli, A. B. Seabra, N. Durán, and O. Rubilar, World J. Microbiol. Biotechnol. **35**, 88 (2019).
[39] R. R. Nayak, N. Pradhan, D. Behera, K. M. Pradhan, S. Mishra, L. B. Sukla, and B. K. Mishra, J. Nanopart. Res. **13**, 3129 (2011).
[40] M. Ahani and M. Khatibzadeh, Micro Nano Lett. **12**, 705 (2017).